International Journal of Engineering and Management Sciences (IJEMS) Vol. 7. (2022). No. 4
DOI: 10.21791/IJEMS.2022.4.4.

The Influence of the Boundary Conditions on the Buckling of Thin-walled Cans during Manufacturing

DÁVID GÖNCZI

University of Miskolc, Faculty of Engineering and Informatics, Institute of Applied Mechanics, mechgoda@uni-miskolc.hu

Abstract. In this paper, the effect of the boundary conditions on the stability of thin-walled aerosol cans under axial pressure is investigated. The main objective is to outline the main characteristics of this highly nonlinear mechanical problem and to present methods to simulate the buckling of cans with different boundary conditions. Due to the numerical difficulties coming from the contact between the can and different components of the machines, the effect of the different supports of the can is investigated on the crushing (or buckling) force at which the loss of stability occurs. The commercial finite element software Abaqus is used to solve the problems and to present the efficiency of FE codes in the design process of cans.

Keywords: cylindrical shell, buckling load, FEM, Abaqus, boundary conditions

Introduction

The global demand of metal packaging product made from mainly pure (99.5%) aluminium or metal is constantly growing. These packaging products are designed to meet the standards of modern design and lifestyle. They come in many shapes and forms and can store a wide variety of products. The packaging can be recycled again and again without loss of quality, making it available today and for the future generations, which makes it the perfect example of a circular economy at work.

A multitude of can sizes, shapes and printing designs can be manufactured to meet individual customer requirements. During the design process of these products, it is important to determine the forming limits of the geometry which is related to the buckling behaviour of the cans. There are several textbooks, that deal with the mechanics of plates and shells, such as [1,2].

Hardy and Abdusslam [3] tackled the numerical simulation of the back extrusion step of thin metal cans. Belblidia et. al. [4], [5] developed finite element techniques to determine the stress state and burst pressure of thin aerosol cans. Article [6] investigated several technological parameters of the forming process of cans using experimental data, while Takeutshi [7] gave a few basic problems in the forming process of thin aluminium cans. Gönczi [8] presented modelling techniques to calculate the reaction forces during the necking phase of the aerosol can manufacturing.

We can find a lot of papers that deal with the loss of stability of different structural components. It is a popular topic to determine the buckling load of beams (such as in [9]) and shells (eg. [10]). Article [11]

DOI: 10.21791/IJEMS.2022.4.4.

investigated specific errors in the geometry, while papers [12-15] introduced the effect of imperfections in specific cases of thin cylindrical shells.

Our aim is to investigate the axial buckling of thin-walled cans and determine the reaction force – displacement functions. To investigate the buckling load, different boundary conditions and different methods to describe the support of the can will be considered. These factors are absent from the previously mentioned works due to the numerical difficulties coming from certain modelling approaches.

1. Model formulation and data

Due to the nature of buckling problems, three-dimensional geometry is used. The can is mapped by thin two-dimensional shell element. It is a highly nonlinear problem, in which large deformations occur. Furthermore the considered material is strain hardened aluminium (99.5%), which involves material nonlinearities. The modulus of elasticity is 75 GPa, the Poisson ratio is 0.4, the yield stress is 120 MPa, moreover a bilinear plasticity law is utilized with 230MPa stress at strain level $\varphi = 4$.

In our problem, there are boundary nonlinearities, which can cause serious numerical issues and errors, moreover they can greatly increase the solution time. One of our main objectives is to present the possibilities to bypass these issues and investigate their effect on the reaction forces, mainly on the buckling force. To support the cans during the shaping process, different tools are used. Figure 1 shows a two-jaw chuck and an eight-jaw chuck used to hold the aerosol cans during necking and bottom forming.

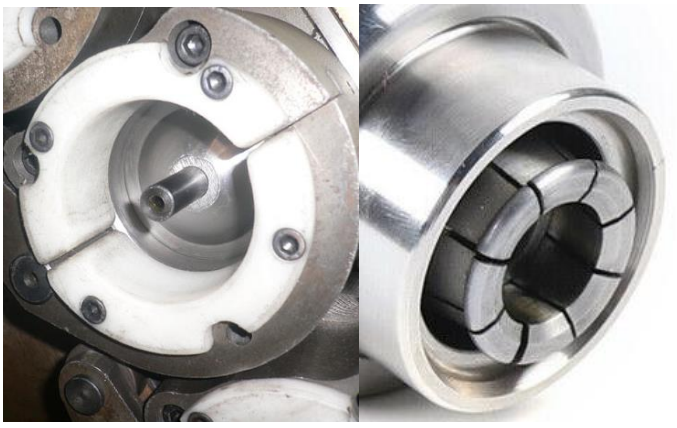

Figure 1. Possibilities for holding thin-walled cans during manufacturing.

At first, the chucks will be replaced by kinematic boundary conditions prescribed at the side and at the base of the cylindrical shell. Then rigid surfaces will be used to support the cans. Finally, three-dimensional continuum element will be used to model the jaws of the chuck to present the efficiency of finite element software to calculate the reaction force – displacement diagram, the stress field and to investigate the different techniques to solve the contact equations.

The initial geometry of cans can be seen in Fig. 2. The length of the can is 200 mm, the diameter is 44 mm, the standard wall thickness is 0.36 mm at the side, 0.9 mm at the base of the cylinder. The dome at the base of the cylinder is R20 mm, the fillet radius is 2 mm.

DOI: 10.21791/IJEMS.2022.4.4.

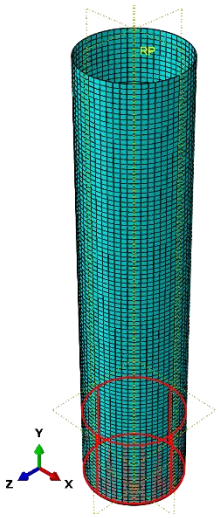

Figure 2. The meshed geometry of the can.

To crush the can and to investigate the reaction forces, the top edge of the shell is tied to a reference point (RP), at which kinematic boundary conditions are prescribed. Here, the degrees of freedom are fixed, except the axial displacement (direction *y*), which is used to deform the can. The other main option to tackle buckling problems is the Riks method.

2. The simplified model

At first, the buckling of the can is investigated using only kinematic boundary conditions and perfect geometry. In the first case, the highlighted area of Fig. 2 is fully pinned, the translational degrees of freedom are fixed, the bottom of the piece is flat. The maximum reaction force (crushing force) is 5920 N. The deformed geometry of the ideal shell can be seen in Fig. 3 with the reaction force – axial displacement diagram (calculated at the reference point of the top of the can).

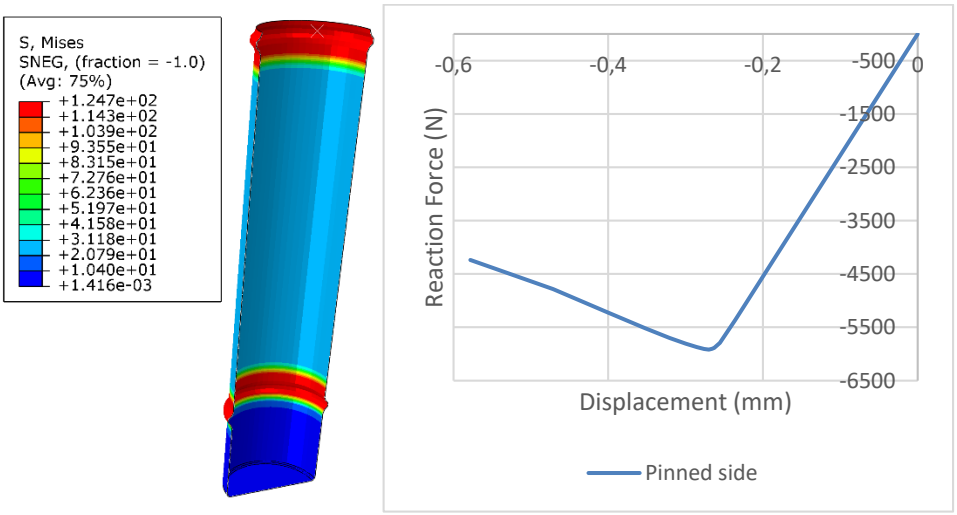

Figure 3. The post buckling shape with the von Mises stresses and the reaction forces of the can with fully pinned side.

DOI: 10.21791/IJEMS.2022.4.4.

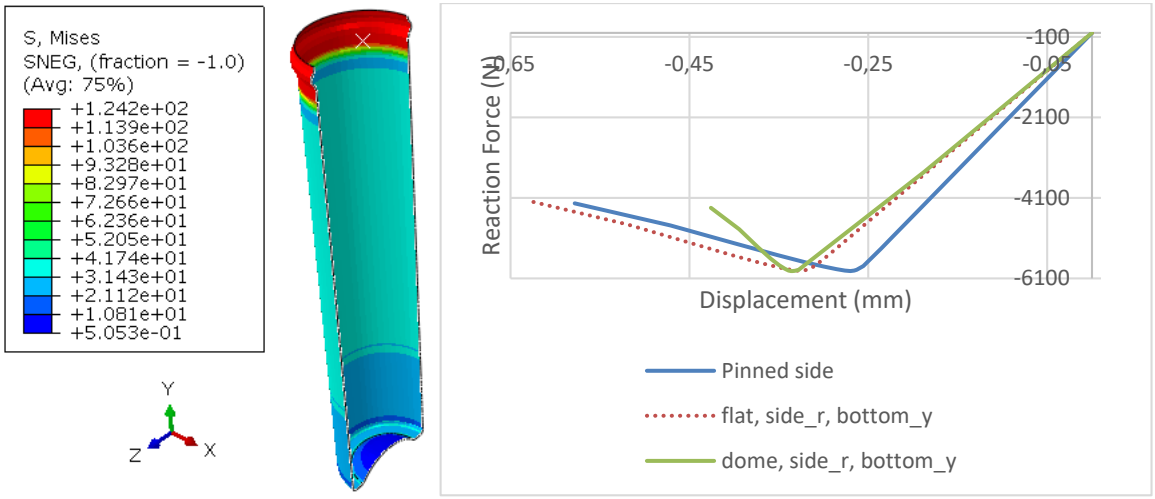

Figure 4. The deformed geometry of the can with a dome and the reaction forces.

In the next case, the aluminium piece is constrained at its bottom against axial displacement (y), at its side of 35 mm height against radial displacement. Here we consider two cases, a can with flat bottom and with a dome, the latter can be seen in Fig. 4 with the reaction forces. The buckling forces (or critical forces) were the same (5920 N). Due to the absence of resistance in the axial direction *y* at the side of the can, the critical displacements (that belong to the critical force) were greater.

3. Contact formulation

To capture the reaction force – displacement curve more accurately, contact zones will be introduced into the model. At first, the contact between the bottom of the can and the support is added, while the side of the can is radially fixed. Hard contact is added in the normal direction, while there is friction at the tangential direction with coefficients: 0.05, 0.3, 0.5. The support is modelled as a discrete rigid surface.

In Abaqus, there are two main options to tackle the contact formulation of this problem. The first one is a surface to surface contact, where the user has to pick the master and slave surfaces using the appropriate meshing considerations. The other is a general contact formulation, in which we can pick additional options to facilitate the calculations, such as contact initialization and stabilization options. Both of these are robust, efficient algorithms and gave results without any major issues.

Figures 5 and 6 show the equivalent stress distributions and the reaction forces coming from the two variants of geometry using different friction coefficients. The critical forces are the same, the critical displacements are different in case of a spherical bottom. Here we note, that in case of small friction coefficients, the critical zone can be the fillet at the base of the can, which causes the change in the reaction force curve in Figs. 5 and 6 for the case of μ=0.05.

DOI: 10.21791/IJEMS.2022.4.4.

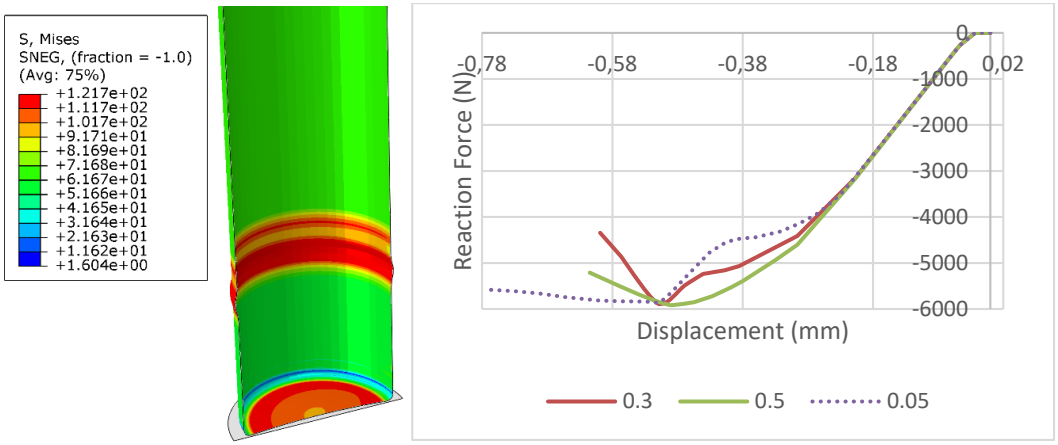

Figure 5. The results of the contact problem at the bottom with initially flat base.

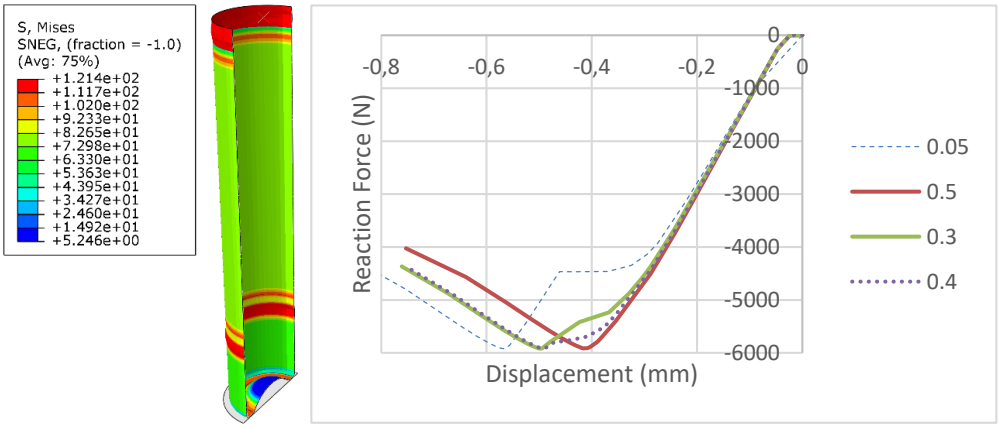

Figure 6. The results of the contact problem with the bottom-dome feature.

In the next phase, the jaws of the chuck is added to the model as discrete rigid surfaces, the rigid support below the can is removed, the flat zone of the bottom of the piece is constrained against axial displacement. Another step is created to investigate the effect of holding the can with two and four jaws (e.g. Fig. 1). The radial force that belongs to the elastic limit (exerted on the individual jaws, where the maximum von Mises stress is just below 120MPa) is 1.38 kN for two jaws, 1.84 kN for four jaws. Figure 7 shows the deformed cans with the two-jaw and four-jaw chucks and the reaction force – displacement diagrams in case of different friction coefficients and jaws.

DOI: 10.21791/IJEMS.2022.4.4.

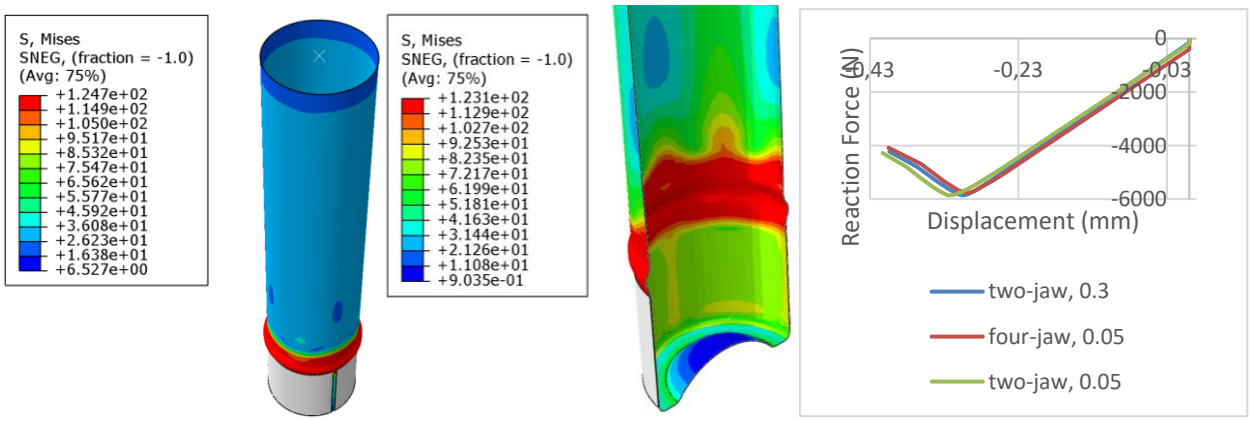

Figure 7. The effect of the rigid jaws.

The deformed geometry with the von Mises stress distribution caused by 4 jaws can be seen in Fig. 8. Here we considered the contact between the bottom of the can and the rigid support surface. As the friction coefficient increases, the critical displacement tends to the axial displacement value of the constrained can (without the bottom support of the previous case). The buckling forces were the same.

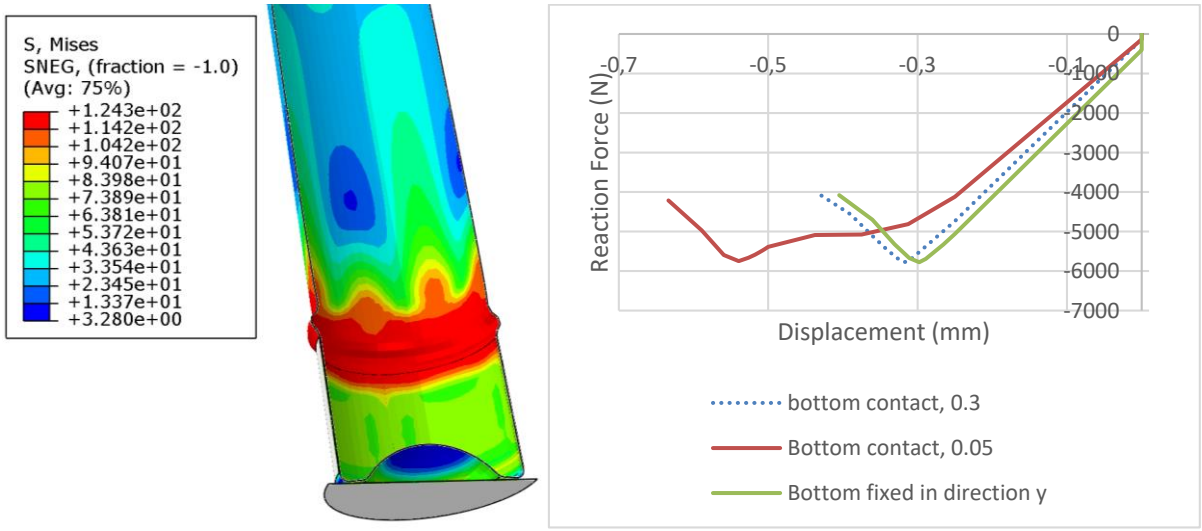

Figure 8. The effect of the combined contact at the bottom and at the side of the can.

Here we note, that according to the contact calculations using rigid jaws, the critical force changes with the increase of the radial force exerted on the jaws. When the radial force 890 N was applied, the maximum von Mises stress in the can was 95 MPa, the critical load 5890 N. At the elastic limit (119.9 MPa) 1.4 kN was used and the buckling force was 5860 N. This decrease in the critical force is insignificant (1%), furthermore in many cases it almost disappears, when we use three-dimensional continuum elements, due to the deformations and the consequent contact pressure distribution caused by the holding system.

DOI: 10.21791/IJEMS.2022.4.4.

4. Implementing continuum elements

In this section, the chuck is modelled as a three-dimensional part meshed with continuum elements. The shell to solid contact formulation of Abaqus is tested and compared to the previously presented simplified models. Figure 9 shows the geometry of the model, the can is supported by an eight-jaw chuck. Two different friction coefficients are investigated ($\mu = 0.05, 0.3$). Here we note, that in reality, the friction coefficient between the support and the can is more, than 0.3, which belongs to the aluminium-aluminium contact. The coefficient of dry steel – aluminium is about 0.4, plastic – aluminium is more, than 0.4. Using different boundary conditions and mechanism to hold the can, the distribution of the contact pressure changes. In Fig. 9 the contact pressure (CPRESS) is illustrated when the base of the chuck is controlled by prescribed radial displacements. This is the reason, why in this case we had more negligible change in the buckling force as the radial holding load increases. It can not cause significant deformations (compared to rigid jaws) in the side of the can above the chuck, which is one of the reasons for the decreased critical force.

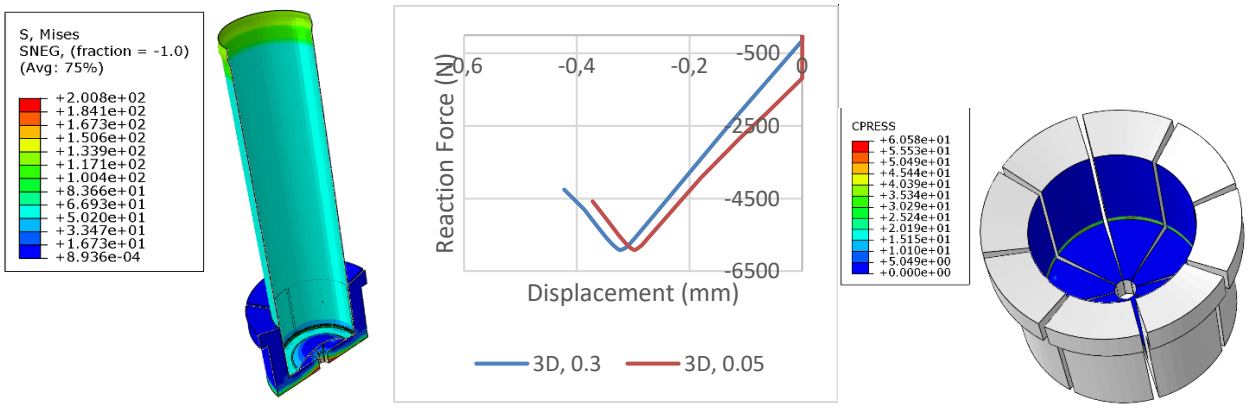

Figure 9. The model with the three-dimensional 8-jaw chuck, different friction coefficients.

In this case, the main area of the contact is just above the fillet of the base, moreover the maximum pressure value is 60 MPa, when the maximum equivalent stress is 119 MPa in the can.

Figure 10 shows the comparison of the previous models. In the presented cases, the friction coefficient was 0.3, the critical loads are approximately the same, moreover the difference between the critical displacements are not significant. Obviously there is a noticeable increase in the critical displacement in the case, when the side is constrained against radial motion while there is a rigid contact between the bottom of the can and the rigid support surface.

DOI: 10.21791/IJEMS.2022.4.4.

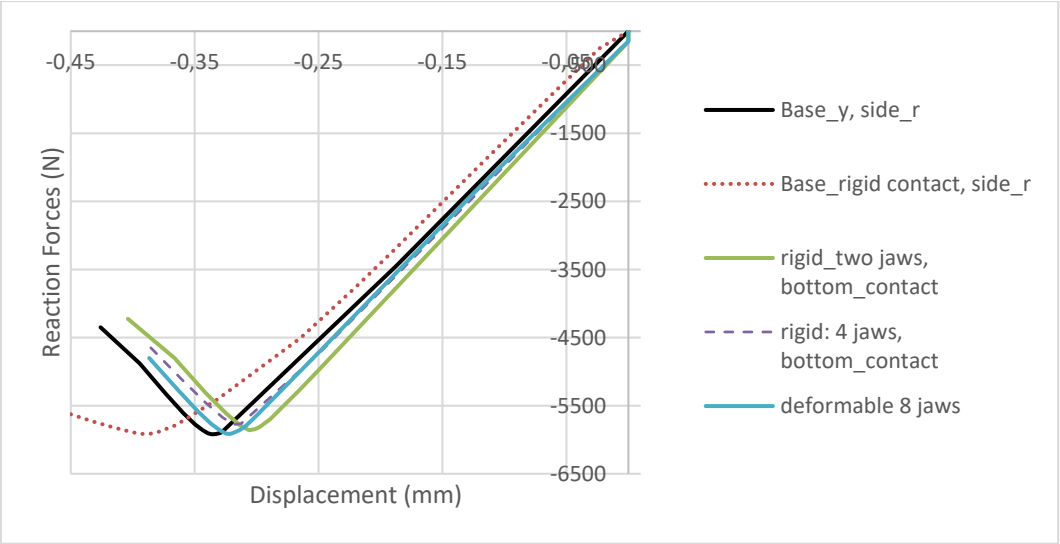

Figure 10. The comparison of the different approaches and boundary conditions.

This means, that the most effective way to model these thin-walled shells during the manufacturing process and buckling analysis is to fix the axial translation of the base of the cylinder while constrain the side against radial motion. Furthermore there were no significant differences between the results coming from different chucks with different number of jaws.

According to experiments, the buckling load is 4% less, than the previously calculated critical force. The difference is the effect comes from the imperfections of the geometry. This effect can cause issues in certain cases, especially for cans with greater tolerance ranges, although in our case the results coming from the ideal geometry were in good agreement with the experiments carried out on quality cans. The other difference is in the post buckling shapes, especially when pure kinematic boundary conditions are used. In reality, the deformed geometry is not axisymmetric, it is based on the errors, or imperfections in the shape of the thin cylinder.

5. Conclusions

This paper investigated the effect of the boundary conditions on the buckling force during the manufacturing process of thin-walled aluminium cans. The geometry was mapped with two-dimensional shell element. At first, the support was modelled as a set of kinematic boundary conditions, then as rigid surfaces and at the end as three-dimensional solid bodies. The paper illustrates the efficiency of finite element method for these highly nonlinear shell problems. The commercial FE software Abaqus was used to calculate the reaction force – displacement diagrams, the stress distributions, the deformations and to tackle contact problems. According to the simulations, the buckling forces were approximately the same, while the critical displacements change. Based on the calculations, a basic combination of certain boundary conditions is proposed to increase the speed of the simulations without significant loss of accuracy in the buckling load.

DOI: 10.21791/IJEMS.2022.4.4.

References

[1] Reddy, J. N. (2006) 'Theory and Analysis of Elastic Plates and Shells'. CRC Press.

[2] Chapelle, D., Bathe, C. J. (2011) 'The Finite Element Analysis of Shells - Fundamentals. 2nd edition', Springer.

[3] Hardy, S. J., Abdusslam, R. M. (2007) 'Finite element modelling of the extrusion process for aluminium aerosol cans', Proc. IMechE, Part L, J. Materials: Design and Applications, 221, pp. 265-274. https://doi.org/10.1243/14644207JMDA153

[4] Belblidia, F., Corft, N., Hardy, S. J., Shakespeare, V., Chambers, R. (2013) 'Simulation based aerosol can design under pressure and buckling loads and comparison with experimental trials', Materials and Design, 52, pp. 214-224. https://doi.org/10.1016/j.matdes.2013.05.041

[5] Belblidia, F., Corft, N., Hardy, S. J. , Bould, D. C. , Sienz, J. (2014) 'Aerosol cans under pressure and buckling loads', Sustainable Design and Manufacturing, 1, pp. 13-17.

[6] Folle, L.F., Netto, S.E.S., Schaeffer, L. (2008) 'Analysis of the manufacturing process of beverage cans using aluminum alloy', Journal of Material Processing Technology, 205, pp. 347-352. https://doi.org/10.1016/j.jmatprotec.2007.11.249

[7] Takeutshi, H. (1993) 'Numerical simulation technology for lightweight aluminium can'. Journal of Material Processing Technology, 38, pp. 675-687. https://doi.org/10.1016/0924-0136(93)90043-6

[8] Gönczi, D. (2020) 'Finite element investigation in the forming process of aluminium aerosol cans', Acta Technica Corviniensis – Bulletin of Engineering, 13(4), pp. 19-22.

[9] Kiss, L. P. (2020) 'Nonlinear stability analysis of FGM shallow arches under an arbitrary concentrated radial force', International Journal of Mechanics and Materials in Design, 16 (1), pp. 91-108.
https://doi.org/10.1007/s10999-019-09460-2

[10] Sofiyev, A. H., Hui, D. (2019) 'On the vibration and stability of FGM cylindrical shells under external pressures with mixed boundary conditions by using FOSDT'. Thin-Walled Structures, 134, pp. 419-427. https://doi.org/10.1016/j.tws.2018.10.018

[11] [11] Prabu, B., Raviprakash, A.V., Venkatraman, A. (2009) 'Neighbourhood effect of two short dents on buckling behavior of thin short stainless steel cylindrical shells'. International Journal of Computer Aided Engineering & Technology, 4(12). https://doi.org/10.1504/IJCAET.2012.045654

[12] Schneider, W. (2006) 'Stimulating equivalent geometrical imperfections for the numerical buckling strength verification of axially compressed cylindrical steel shells'. Computational Mechanics, 37(6), pp. 530-536. https://doi.org/10.1007/s00466-005-0728-8

[13] Guggenberger, W. (1995) 'Buckling and postbuckling of imperfect cylindrical shells under external pressure', Thin Walled Structures, 23, pp. 351–366.

DOI: 10.21791/IJEMS.2022.4.4.

[14] Holst, F. G., Rotter, J. M., Calladine, C. R. (1994) 'Imperfections in cylindrical shells resulting from fabrication misfits', Journal of Engineering Mechanics, 125(4), pp. 410–418.

[15] Kiss, L. P., Gönczi, D., Baksa, A., Kovács, P. Z., Lukács, Zs. (2020) 'Experimental and numerical investigations on the stability of cylindrical shells', *Journal of Engineering Studies and Research*, 26(4), pp. 34-39.

[16] Kiss, L. P. (2020) 'The effect of various imperfections on the buckling of aluminium shells', *Acta Technica Corviniensis – Bulletin of Engineering*, 13(1), pp. 49- 52.